Modelling excitable cells using cycle-linear hybrid automata

P. Ye, E. Entcheva, S.A. Smolka and R. Grosu

Abstract: Cycle-linear hybrid automata (CLHAs), a new model of excitable cells that efficiently and accurately captures action-potential morphology and other typical excitable-cell characteristics such as refractoriness and restitution, is introduced. Hybrid automata combine discrete transition graphs with continuous dynamics and emerge in a natural way during the (piecewise) approximation process of any nonlinear system. CLHAs are a new form of hybrid automata that exhibit linear behaviour on a per-cycle basis but whose overall behaviour is appropriately nonlinear. To motivate the need for this modelling formalism, first it is shown how to recast two recently proposed models of excitable cells as hybrid automata: the piecewise-linear model of Biktashev and the nonlinear model of Fenton−Karma. Both of these models were designed to efficiently approximate excitable-cell behaviour. We then show that the CLHA closely mimics the behaviour of several classical highly nonlinear models of excitable cells, thereby retaining the simplicity of Biktashev's model without sacrificing the expressiveness of Fenton−Karma. CLHAs are not restricted to excitable cells; they can be used to capture the behaviour of a wide class of dynamic systems that exhibit some level of periodicity plus adaptation.

1 Introduction

Hybrid automata [1] are an increasingly popular modelling formalism for systems that exhibit both continuous and discrete behaviour. Intuitively, a hybrid automaton is an extended finite-state automaton, the states of which encode the various phases of continuous dynamics a system may undergo and the transitions of which are used to express the switching logic between these dynamics. Hybrid automata are well suited as a computational model for continuous−discrete systems as they (i) possess an intuitive graphical representation, (ii) can be used in a natural way to achieve a piecewise, possibly linear, approximation of any nonlinear system and (iii) facilitate formal analysis due to their automata-theoretic nature.

Traditionally, hybrid automata have been used to model embedded systems, including automated highway systems [2, 3], air traffic management [4, 5], embedded automotive controllers [6], robotics [7] and real-time circuits [8]. More recently, they are being applied to formally model molecular, intra-cellular and inter-cellular biological processes [9]. Many biological systems are 'hybrid' in nature: biochemical concentrations may vary continuously, yet discrete transitions between distinct states are also possible.

Excitable cells are a good example of hybrid biosystems: transmembrane ion fluxes and voltages may vary continuously but the transition from the resting state to the excited state is generally considered an all-or-nothing discrete response. Furthermore, networks of genes, molecules and cells tend to exhibit properties such as concurrency and communication, for which automata-based formalisms are well developed [10].

Currently, the preferred modelling approach for biological systems uses large sets of coupled nonlinear differential equations, and analysis is reduced to simulation via numerical techniques. In contrast, models based on hybrid automata provide piecewise, typically linear, approximations, which lead to conceptually simpler models and the possibility for large-scale simulation and formal analysis.

In this paper, we introduce cycle-linear hybrid automata (CLHAs), a novel model for excitable cells that efficiently and accurately captures both action-potential (AP) morphology and typical excitable-cell characteristics such as refractoriness and restitution. The CLHA formalism is motivated by the distinct modes observed during an AP − resting, stimulated, early repolarisation and final repolarisation. During each one of them, the dynamics of the system is essentially linear and time-invariant (LTI). To capture frequency-dependent properties such as restitution, the CLHA model can be equipped with memory of the cell's voltage, and the per-mode parameters of the current cycle's LTI system of differential equations are updated according to this voltage. Consequently, the model's behaviour is linear in any one cycle but appropriately nonlinear overall.

To motivate the need for CLHA, we first show how to recast two recently proposed models of excitable cells as hybrid automata: the piecewise-linear model of Biktashev [11] and the nonlinear model of Fenton−Karma [12]. Both of these models were designed to efficiently approximate excitable-cell behaviour. We then show that our CLHA model closely mimics the behaviour, in terms of AP morphology and frequency-dependent restitution, of several classical highly nonlinear models of excitable cells: the Hodgkin−Huxley model of an axon [13], and two models of cardiac myocytes − the dynamic Luo−Rudy model [14] and a neonatal rat model, which we

P. Ye, S.A. Smolka and R. Grosu are with Computer Science Department, SUNY at Stony Brook, Stony Brook, NY 11794, USA

E. Entcheva is with Biomedical Engineering Department, SUNY at Stony Brook, Stony Brook, NY 11794, USA

E-mail: iyepei@gmail.com

shall henceforth refer to as HH, LRd and NNR, respectively. One may thus conclude that CLHA, as a formal model of excitable cells, retains the simplicity of Biktashev's model without sacrificing the expressiveness of Fenton–Karma.

CLHAs are not restricted to excitable cells; they can be advantageously used to model any dynamical system that exhibits some level of periodicity plus adaptation. A preliminary version of this paper appeared in [15]; see also [16, 17].

The rest of the paper is organised as follows. Section 2 discusses the related work. Section 3 defines hybrid automata. Section 4 provides the requisite biological background for excitable cells. Section 5 shows how to recast the existing computational models of excitable cells as HA using the Heaviside function for discrete control. Section 6 presents our CLHA model, and Section 7 shows how it can be used to efficiently model the AP and associated frequency-dependent properties of different excitable cells. Section 8 summarises this work and discusses the future research.

2 Related work

As discussed in the previous section, HA are finding more and more use as a modelling formalism for molecular, intracellular and inter-cellular biological processes. In [9], an HA model of a protein-regulatory network is derived by identifying the major modes of operation and the manner in which the network switches between modes. Each of two interacting proteins is associated with two modes: active and non-active. In each mode, a linear dynamic function is used to describe the concentration change of that protein. HA models constructed in this fashion tend to be of low complexity as well as low precision, but may facilitate large-scale simulation and analysis.

Alternatively, a system of coupled nonlinear ordinary differential equations (ODEs) describing processes with disparate time scales can be simplified and transformed into an HA model. This is the approach considred by Biktashev [11], where a Heaviside function is substituted for a fast-transitioning continuous function, along with certain assumptions about variables remaining constant within a mode [11].

Antoniotti *et al.* [18] advocate an empirical approach to derive HA models of biochemical systems from experimental data. In their approach, each time step is associated with a mode. If the data set is large, so is the resulting automaton. Simplification techniques based on 'state collapsing' can be used to reduce the number of states, making this method feasible for real applications.

Once an HA model has been developed for a biological system, it can be used to explore the system's parameter space. Moreover, because of their abstract nature (relative to nonlinear systems), HA admit the possibility of formal systems analysis. Of particular interest for dynamical systems are reachability and stability analysis. The former allows one to check whether the transient behaviour of an HA contains undesired modes of operation [19, 20]. The latter allows one to check whether the HA, in steady state, exhibits unstable (or chaotic) behaviour [21, 22]. The information gleaned from these forms of analysis can be exploited to control the system in question such that it stays within desired limits.

3 Hybrid automata

Intuitively, an HA is an extended finite-state automaton, where each state is endowed with a continuous dynamics

[1]. Formally, an HA $\mathcal{A} = (X, G, \text{init}, \text{inv}, \text{flow}, \text{jump}, \text{event})$ over finite set $\sum$ of events is a 7-tuple, whose components are as follows:

- A finite set X of real-valued variables $x_1, \ldots, x_n$; their dotted form $\dot{x}_i \in \dot{X}$ represents the first derivatives and their primed form $x'_i \in X'$ represents the values at the conclusion of discrete steps (jumps); n is called the dimension of $\mathcal{A}$.
- A finite control graph $G = (V, E)$, where vertices in V are called modes and edges in E are called switches.
- For each mode $v \in V$, vertex-labelling functions init, inv and flow with domain V and range P, where P is the set of all logical predicates. Initial condition init(v) and invariant inv(v) are predicates with free variables from X. Flow flow(v) is a predicate with free variables from $X \cup \dot{X}$ representing a set of ordinary (partial) differential (in)equalities.
- A finite set $\sum$ of events which are essentially binary variables controlled from outside the system, and an edge-labelling function event: $E \rightarrow \sum$ that assigns to each switch an event.
- Edge-labelling functions jump: $E \rightarrow$ (Guard, Action), where Guard is the set of predicate with free variables from $X \cup \sum$ and Action is the set of assignments that update the variables in X'.

Intuitively, $\mathcal{A}$ spends time in its modes $v \in V$, where it updates its variables according to the flow predicate flow(v). Jumps jump(e) on switches $e = (v, w)$ are in contrast instantaneous, where v is the beginning mode and w is the end mode of the switch. A jump on e is taken whenever the jump's guard jump(e).guard is enabled for the current values of variables X, or the invariant of the current mode inv(v) is unsatisfied.

We shall subsequently restrict our attention to HAs for which flows are defined by differential equalities (rather than inequalities) and for which jumps are deterministic. Determinism in the definition of the jumps here means that if a mode is a source of multiple jumps, always at most one of the guards of these jumps evaluates to 'true'.

An HA has a natural graphical representation as a state-transition diagram, with control modes as the states and control switches as the transitions. Flows and invariants (predicates within curly braces) appear within control modes, while jump conditions (in square brackets) and actions appear near the control switches. We shall use lower-case alphabets, such as x, y, v, and possibly v_x, v_y and so on, to denote continuous variables.

As an example, consider HA $\mathcal{A}$ in Fig. 1, which models a simple thermostat system. $\mathcal{A}$ is a 1-dimensional system with $X = \{x\}$, where x represents the current temperature. Also, $G = (\{\text{ON, OFF}\}, \{(\text{ON, OFF}), (\text{OFF, ON})\})$, inv(OFF) = $\{x \geq 18\}$, inv(ON) = $\{x \leq 22\}$, flow(OFF) = $\{\dot{x} = -0.1x\}$, flow(ON) = $\{\dot{x} = 5-0.1x\}$, jump((OFF, ON)).Guard = $\{x > 21\}$, jump((ON, OFF)).Guard = $\{\text{TurnOn} \vee x < 19\}$, $\sum = \{\text{TurnOn}\}$, event((OFF, ON)) = TurnOn. Initially, $\mathcal{A}$ is in mode OFF with x initialised to 20°C. While in this mode, the heater is off and the temperature drops. Then the system has two possibilities after the temperature reaches 19°C. It can either switch to mode ON or stay in
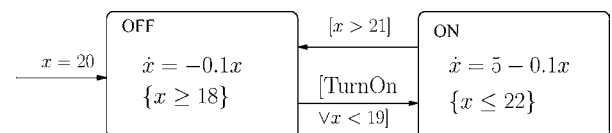
Fig. 1 *Thermostat system modelled as an HA*

IET Syst. Biol., Vol. 2, No. 1, January 2008

25

mode OFF until the temperature falls below 18°C when the system is forced to leave mode OFF. This is where non-determinism can be modelled in HA. Another cause for the system switching from OFF to ON is when the event TurnOn happens. The occurrence of this event means that the heater has been manually turned on, causing $\mathcal{A}$ to jump to mode ON. In mode ON, the heater is on and the temperature rises until it is above 22°C. Or it can jump to mode OFF when the temperature is above 21°C, in a similar manner as we discussed above.

4 Excitable cells

Excitable cells include neurons, cardiac cells, skeletal cells and smooth muscle cells. For cardiac cells, on each heart beat, an electrical control signal is generated by the sinoatrial node, the heart's internal pacemaking region. Electrical waves then travel along a prescribed path, exciting cells in the main chambers of the heart (atria and ventricles) and assuring synchronous contractions. At the cellular level, the electrical signal is a change in the potential across the cell membrane which is caused by different ion currents flowing through the cell membrane. This electrical signal for each excitation event is known as an AP. Fig. 2 shows the AP waveform for a guinea-pig ventricular cell.

For non-pacemaking excitable cells, APs are externally triggered events: a cell fires an AP as an all-or-nothing response to a supra-threshold stimulus, and each AP follows the same sequence of phases and maintains approximately the same magnitude regardless of the applied stimulus. After an initial step-like increase in the membrane potential, an AP lasts for a couple of milliseconds to hundreds of milliseconds in most mammals. During an AP, generally no re-excitation can occur. The early portion of an AP is known as the 'absolute refractory period' due to its non-responsiveness to further stimulation. The later portion is known as the 'relative refractory period', during which an altered secondary excitation event is possible if the stimulation strength or duration is raised.

When an excitable cell is subjected to repeated stimuli, two important time periods can be identified: the AP (APD), the time the cell is in an excited state, and the diastolic interval (DI), the time between the end of the AP and the next stimulus. Fig. 2 illustrates the two intervals. The function relating APD to DI with change in stimulation frequency is called the APD restitution function. As shown in Fig. 3, the relationship is nonlinear and captures the phenomenon that a longer recovery time is followed by a longer APD. A physiological explanation of a cell's
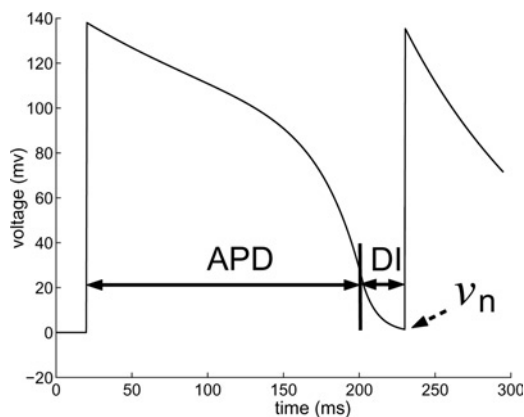
Fig. 2 *AP and its APD and DI time periods*
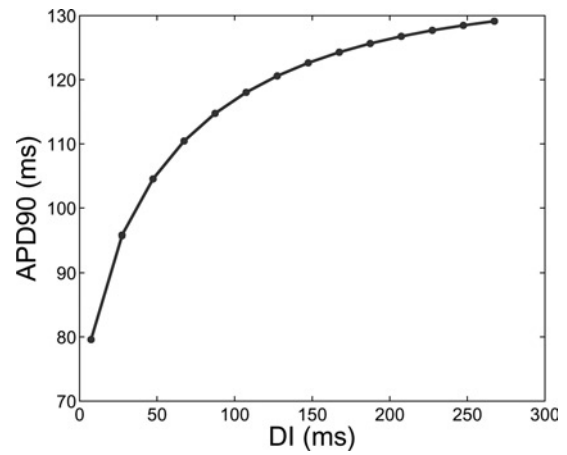
Fig. 3 *APD dependence on DI in the LRd model*

restitution is rooted in the ion-channel kinetics as a limiting factor in the cell's frequency response.

5 Models of excitable cells as HAs

During the early stages of the quest for models of excitable cells amenable to analytical investigation, FitzHugh and Nagumo proposed an approximate model of excitable cells [23-24], referred to here as the FHN model. With their model, they showed that a modified version of the Van der Pol oscillator with two state variables can mimic the essential features of the HH dynamics.

Subsequently, a piecewise-linear version of the FHN model was proposed by McKean [25] which used a Heaviside function to represent switches between linear regimes or modes. Since then, the Heaviside function has been used in different simplified renditions of excitable-cell models to achieve piecewise control.

5.1 From Heaviside Control to HAs

Discrete transitions in system behaviour, such as those captured by Heaviside functions, are an integral part of the HA formalism. Let S be a dynamic system defined using the Heaviside function. We present a systematic way to transform S into an equivalent HA. The Heaviside function $H(x)$ is a discontinuous function defined as follows

$$H(x) = \begin{cases} 0, & x < 0 \\ 1, & x \geq 0 \end{cases} \quad (1)$$

Assuming that the state equation of S has the structure of (2), where $\vec{v}$ is a vector of state variables x, it is straightforward to show that S is equivalent to the HA shown in Fig. 4.

$$\dot{v} = f(H(x), y), \quad \vec{v} = (x, \vec{y}) \quad (2)$$

One can generalise the above translation to any dynamic system whose state equations are defined using Heaviside functions. In the following, we apply this translation to two recently proposed approximate models for
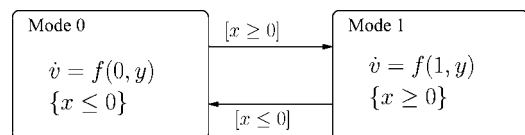
Fig. 4 *Heaviside function recast as an HA*

26

IET Syst. Biol., Vol. 2, No. 1, January 2008

cardiac-tissue excitability: the piecewise-linear model of Biktashev [11] and the nonlinear model of Fenton and Karma [12].

5.2 Biktashev's model

The increasing complexity of excitable-cell models describing AP morphology with large sets of state variables and nonlinear differential equations triggered continuous efforts to obtain simplified descriptions that preserve important properties.

Biktashev made the observation that the widely used FHN model is not sophisticated enough to capture the propagation failure due to dissipation of the wavefront, a phenomenon seen in more realistic models [11]. This was attributed to the more phenomenological nature of the FHN model, which was not directly derived from the original HH model, but rather devised to mimic its properties. Instead, a formal derivation procedure was proposed based on singular perturbation theory developed by Tikhonov [26] and Pontryagin [27]. The procedure reduces the size of the differential equations by taking advantage of the fast–slow nature of the system, that is, by separating the state variables into two groups, fast–slow, and by linking the two sets of equations via a perturbation parameter. The model thus obtained was able to overcome the above-mentioned deficiency of the original FHN model. Furthermore, its simplicity allowed analytical treatment [11, 28, 29].

Consider Biktashev's simplified model [11], where H is the Heaviside function, E the transmembrane voltage, h the probability density of a sodium-channel gate being open, D the (constant) diffusion coefficient and τ also constant. $\dot{E}$ and $\dot{h}$ are the time derivatives of state variables E and h and $\nabla(D\nabla E)$ is the second-order directional derivative on the 2D space, representing the diffusion factor when modelling the spatial propagation of cell excitations.

$$\dot{E} = \nabla(D\nabla E) + H(E-1)h \tag{3}$$

$$\dot{h} = \frac{1}{\tau}(H(-E) - h) \tag{4}$$

From the prespective of one cell, $\nabla(D\nabla E)$ is the (input) stimulation current I_s produced by neighbouring cells. Hence, (3) can be rewritten as follows: $\dot{E} = I_s + H(E-1)h$. Applying the transformation process for systems employing Heaviside control (Section 5.1) yields the 3-mode HA shown in Fig. 5, with each mode having flows described by LTI differential equations.

The linearity of the flows is clearly an advantage of this model, as it supports efficient simulation and detailed analysis. However, the simplicity of Biktashev's model comes at a price: the inability to faithfully reproduce AP morphology, as discussed in [11, 29]. This is probably due to the treatment of τ as a constant, when in reality it is a voltage-dependent parameter that can vary over a relatively wide range. Recently, this piece-wise linear formulation has been augmented with non-Tikhonov asymptotic reduction to obtain a more realistic AP morphology. For example, Biktashev started with the Courtemanche model of the

atrial heart cell [30] and applied asymptotic embedding, considering fast and slow variables, to obtain a reduced system [29, 31]. The resultant model captures AP morphology well, but is nonlinear in each of the modes separated by a Heaviside function.

5.3 Fenton–Karma model

Fenton and Karma [12] proposed a three-variable ionic model as a substitute for the full ionic LRd-type models, by grouping the various ion currents into three generic ones: fast inward current I_{fi}, slow inward current I_{si} and slow outward current I_{so}. The corresponding three-variable model given below [(5)–(11)] contains dynamic functions for the normalised membrane voltage u, inactivation–reactivation gate v for I_{fi} and gate w for I_{si}

$$\dot{u} = \nabla \cdot (\widetilde{D}\nabla u) - J_{fi}(u;v) - J_{so}(u) - J_{si}(u;w) \tag{5}$$

$$\dot{v} = \frac{H(u_c - u)(1-v)}{\tau_v^-(u)} - \frac{H(u - u_c)v}{\tau_v^+} \tag{6}$$

$$\dot{w} = \frac{H(u_c - u)(1-w)}{\tau_w^-} - \frac{H(u - u_c)w}{\tau_w^+} \tag{7}$$

$$J_{fi}(u;v) = -\frac{v}{\tau_d}H(u - u_c)(1-u)(u-u_c) \tag{8}$$

$$J_{so}(u) = \frac{u}{\tau_o}H(u_c - u) + \frac{1}{\tau_r}H(u - u_c) \tag{9}$$

$$J_{si}(u;w) = -\frac{w}{2\tau_{si}}(1 + \tanh[k(u - u_c^{si})]) \tag{10}$$

where $J_{fi}(u;v)$, $J_{si}(u;w)$ and $J_{so}(u)$ are the normalised versions of $I_{fi}(u;v)$, $I_{si}(u;w)$ and $I_{so}(u)$, respectively, u_c and u_c^{si} the thresholds for activation of I_{fi} and I_{si}, and τ_v^+, τ_w^-, τ_w^+, τ_d, τ_o, τ_r and τ_{si} the time constants

$$\tau_v^-(u) = H(u - u_v)\tau_{v_1}^- + H(u_v - u)\tau_{v_2}^- \tag{11}$$

$\tau_v^-(u)$ is further defined by the Heaviside function of (11), where u_v is the threshold potential and $\tau_{v_1}^-$ and $\tau_{v_2}^-$ the time constants.

The Fenton–Karma model recast as an HA is shown in Fig. 6, where the HA was derived by taking into account the definition of the Heaviside functions.
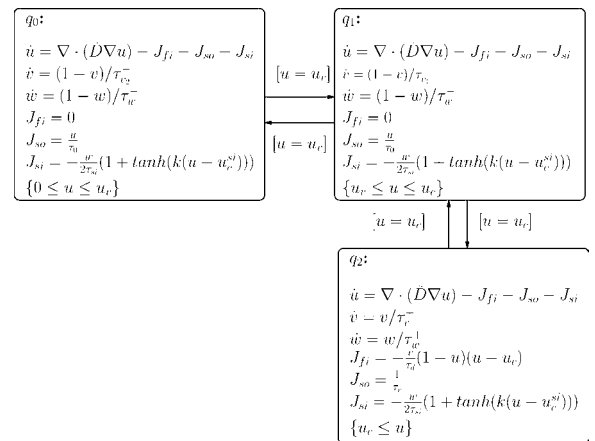
Fig. 6 *HA for the Fenton–Karma three-variable, three-ion-current model*

Fig. 5 *Biktashev's model in the HA framework*

IET Syst. Biol., Vol. 2, No. 1, January 2008

27

The Fenton–Karma model has the flexibility to match AP morphology by correct selection of the parameters, possibly via an optimisation procedure. It also has been shown to properly model restitution properties of other more complex models or empirically obtained data. However, similar to Biktashev's asymptotically reduced models, the resultant simplified system is still nonlinear and therefore not particularly well suited to analytic treatment.

6 CLHA for excitable cells

In Section 5, we saw that the computational models of excitable cells employing the Heaviside function for discrete control can be recast as an HA. In particular, Biktashev's simplified model [11] corresponds to an LTI-HA: an HA having LTI flows in each mode. An LTI-HA, such as Biktashev's, is amenable to efficient numerical (or event-driven [32]) simulation as well as formal analysis. Biktashev's simplified model and the corresponding HA are, however, unable to faithfully capture AP morphology.

Biktashev's more sophisticated models and the Fenton–Karma model correspond to HA having nonlinear flows in at least one mode and faithfully capture AP morphology and restitution properties. Because of the nonlinearity present in these models, however, HA simulation is less efficient, and powerful analysis techniques developed for linear systems are not directly applicable.

Given this state of affairs, we propose CLHAs as a new HA-based formalism for modelling excitable cells. The CLHA formalism was designed to be both (i) abstract enough to admit formal analysis and efficient simulation and (ii) expressive enough to capture the AP morphology and restitution properties exhibited by classical, nonlinear excitable-cell models (HH, LRd and NNR, in particular).

The basic idea behind the CLHA model is the observation that, during an AP, an excitable cell cycles through four basic modes of operation – resting, stimulated, upstroke, early repolarisation, plateau final repolarisation – and the dynamics of each mode is essentially LTI. Thus, on a per-cycle basis, a CLHA can be viewed as an LTI-HA. To capture possibly nonlinear, frequency-dependent properties such as restitution, the CLHA model is equipped with a one-cycle memory of the cell's voltage – in particular, the value of the cell's voltage when it was last subjected to an outside stimulus – and the per-mode parameters of the current cycle's LTI system of differential equations are updated according to this voltage. Consequently, the model's behaviour is linear in any one cycle but appropriately nonlinear overall.

6.1 CLHA derivation method

The method we used to derive the CLHA model for excitable cells focuses on the following three issues.

Topology. The topology of a CLHA refers to the design of its control graph, that is, the control graph's modes and switches.
Flows. Let $\mathcal{A}$ be a CLHA defined over a set (vector) of state variables X. The dynamics of $\mathcal{A}$ is determined by the dimension of X and, for each mode q of $\mathcal{A}$, the form of q's flow (system of ODEs in X).
Adaptability. This refers to the mechanism built into the CLHA model that allows it to exhibit stimulation-frequency adaptability. This feature is essential for the successful modelling of AP morphology and restitution.

The discussion of our derivation method proceeds as follows. We first consider topology and flows and in the process derive an LTI-HA model $\mathcal{A}_1$ that approximates the AP trajectory of one representative AP cycle of an excitable cell. Since for one AP cycle we are able to use LTI flows in each mode, $\mathcal{A}_1$ is an LTI-HA. We then turn our attention to adaptability. In the process, we derive our final CLHA model $\mathcal{A}_2$, which offers an accurate approximation of the (infinite-trajectory) phase space of the original nonlinear system by introducing a memory unit into LTI-HA $\mathcal{A}_1$. Finally, we give the formal definition of the CLHA model.

6.1.1 Topology: The choice of modes for both our LTI-HA $\mathcal{A}_1$ and CLHA $\mathcal{A}_2$ models is inspired by the fact that although the AP for different cell types (neuron, cardiac myocyte, etc.) or different species (guinea pig, NNR, etc.) exhibits different waveforms, when observed over time, one can universally identify the following phases within a cycle: resting, upstroke, early repolarisation, plateau or later repolarisation and final repolarisation. Fig. 7a shows a typical AP cycle for a guinea pig ventricular cell. The voltage thresholds V_T, V_O and V_R serve to delineate one phase of the AP cycle from another.

For the purpose of mode identification, we are also interested in the period of time when an excitable cell is stimulated and can be further subjected to external stimulation. We shall refer to this mode as stimulated and allow the CLHA model to accept input within this mode. This leads us to the following choice of four modes for our CLHA model in order to cover the complete AP cycle: stimulated (ST), upstroke (UP), early repolarisation and plateau (EP) and final repolarisation and resting (FR).

As illustrated in Fig. 7b, where flows are momentarily ignored, the mode transition relation for $\mathcal{A}_1$ and $\mathcal{A}_2$ is generally cyclic in nature, although we allow the cell to return to mode FR from mode ST when it is under insufficient stimulus.

Because of its topology, $\mathcal{A}_1$ and $\mathcal{A}_2$ already possess two common features of excitable cells: absolute refractoriness and graded response to sub-threshold stimulation. Regarding the former, once a cell is excited, for example with a stimulus current, it enters an absolute refractory period, where the cell is non responsive to further excitation. This is reflected in our models by modes UP and EP, during which no further input is accepted and the cell cannot return to mode UP. Another excitation is possible only when the cell is in FR and is captured with by a begin-stimulation event e_s that moves the model to mode ST.

Graded response to sub-threshold stimulation manifests in mode ST, where a cell accumulates its membrane voltage by accepting an input current. As soon as its voltage exceeds threshold V_T, the cell moves to mode UP. Otherwise, should the end-stimulation event $\bar{e}_s$ occur while $v < V_T$, the cell returns to mode FR. The cell
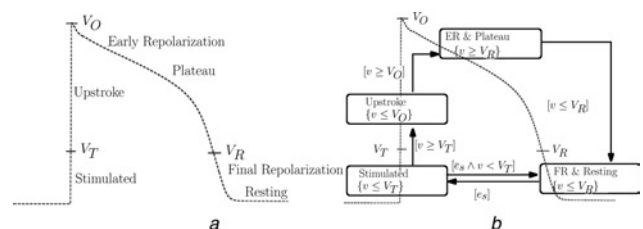
Fig. 7 *Typical AP cycle and structure of CLHA*
a Major AP phases
b Structure of CLHA model

returning to the resting phase is ultimately a consequence of the refractory modes: if the stimulus occurs at a sufficiently high pace, the second stimulation event may be missed.

The physiological separation of modes (or phases) of the AP has been our guiding principle for mode identification in our HA models. Recently, however, we have investigated the automated splitting of modes based on mathematical properties of AP waveforms other than their physiological meaning [33]. In the case of mode ST, there are two situations. In the single-cell case, since the outside stimulus can be specified before simulation begins, events e_s and $\overline{e}_s$ are well defined. In spatial simulations, where a cell may also accept stimuli from its neighbours, events e_s and $\overline{e}_s$ represent, respectively, the abstraction of the process of the cell sensing its neighbours' potential and subsequently deciding to fire. Although the use of these events in the spatial setting may seem somehow arbitrary, spatial simulations using the HA models are both efficient and capable of reproducing re-entry waves in cardiac tissues. HA-based spatial simulation is discussed in a separate paper [15].

6.1.2 Flows: The basic idea behind the flows of LTI-HA $\mathcal{A}_1$ is to capture the nonlinear dynamics (morphology) of a single AP in a piecewise-linear fashion. Since the AP (voltage v) is the only observed variable and we do not have other constraints on the dynamics of state variables, the flows in each mode can be described in a purely linear manner as follows

$$\dot{X} = AX \tag{12}$$

$\dot{X}$ is the first derivative of X with respect to time and A is a constant diagonal matrix. Thus, the only interdependencies among the state variables is through the observable v. Regarding the system's dimension, the greater the number of state variables, the greater is its precision, with the complexity of the system description increased as well. We choose here to use three state variables, v_x, v_y and v_z, as a balance between precision and system complexity, with the overall membrane voltage v defined as follows

$$v = v_x - v_y + v_z \tag{13}$$

Let $A = \text{diag}(\alpha_x, \alpha_y, \alpha_z)$. The flows in modes UP, EP and FR, where no input is accepted, are given by

$$\dot{v}_x = \alpha_x v_x, \quad \dot{v}_y = \alpha_y v_y \quad \dot{v}_z = \alpha_z v_z \tag{14}$$

As discussed in detail in Section 7, curve-fitting techniques are used on a mode-by-mode basis to determine parameters α_x, α_y and α_z such that $\mathcal{A}_1$s output, that is, the AP v, reproduces up to a prescribed error margin the AP of the original nonlinear system.

Considering a linear dependence on the input in mode ST, we still remain within the LTI-HA framework, but are now able to capture a (simplified) family of related trajectories

$$\dot{v}_x = \alpha_x v_x + \beta_x I_s, \quad \dot{v}_y = \alpha_y v_y + \beta_y I_s,$$
$$\dot{v}_z = \alpha_z v_z + \beta_z I_s \tag{15}$$

As in the other modes, α_x, α_y and α_z and β_x, β_y and β_z are the constants to be fitted.

6.1.3 Adaptability: The shape of the AP generated by $\mathcal{A}_1$ is fixed by the constant (matrix and scalar) parameters α, β, V_T, V_O and V_R. Moreover, the APD depends solely on the stimulation frequency, as the time $\mathcal{A}_1$ spends in modes ST, UP and EP (for fixed amplitude of I_s) is constant.

In contrast, the original nonlinear system has a phase space comprising infinitely many trajectories. To obtain an accurate approximation of this space, we derive CLHA $\mathcal{A}_2$ from $\mathcal{A}_1$ by generalising $\mathcal{A}_1$s constant parameters α, β, V_O and V_T to cycle-constant functions $\boldsymbol{\alpha}(\theta)$, $\boldsymbol{\beta}(\theta)$, $V_O(\theta)$ and $V_T(\theta)$, where θ is a normalised, one-cycle memory of the voltage. The derivation of $\mathcal{A}_2$ from $\mathcal{A}_1$ is based on the following observations:

• APs in different cycles share a similar morphology. It should thus be possible to to model them using equations possessing the same structure.
• According to the restitution property, AP morphology is principally determined by the length of the previous DI. This indicates that a control strategy based on a relatively simple, single-step memory unit will suffice for adaptability purposes.

CLHA morphology. The DI in one AP-cycle influences the shape of the AP in the next cycle, in particular, the APD, stimulation voltage V_T and overshoot voltage V_O. The time $\mathcal{A}_2$ spends in modes ST and UP is relatively small compared with the APD, therefore allowing the influence of the DI in these modes to be ignored. The time $\mathcal{A}_2$ spends in modes FR and EP, however, can be considerable.

CLHA memory. One can accurately model the DI by introducing a timer (a variable whose derivative with respect to time is 1) that is reset when $\mathcal{A}_2$ enters mode FR and measured when the stimulation event e_s occurs. To avoid the introduction of a new state variable into the model, we choose instead to linearly approximate the DI with the value of $\mathcal{A}_2$s voltage v upon the occurrence of e_s. We remember this value by introducing a discrete variable v_n that is updated on the transition from FR to ST by the (assignment) action $v'_n = v$. (Note that v_n is 'discrete' in the sense that its derivative is zero in all modes. This is in contrast to the term's traditional meaning: that of a variable whose range of possible values is discrete.)

Let $\theta = v_n/V_R$ and recall that the invariant of mode FR is $v \leq V_R$. We thus have that $0 \leq v_n \leq V_R$, and therefore θ is a normalised approximation of DI

To see why the normalized v_n is a linear approximation of the DI, consider the triangles of Fig. 8. According to the similar triangles property, we have $(V_R - v_n)/V_R = \text{DI}/\text{DI}_m$. As $\theta = v_n/V_R$, we have $\text{DI} = \text{DI}_m(1 - \theta)$. Thus the previous DI is approximated in a linear way by θ

As the AP morphology is controlled by previous DI, we therefore make the parameter matrix $\boldsymbol{\alpha}$ a function of θ by introducing the cycle-constant parameter matrix $\overline{\boldsymbol{\alpha}}$ such that

$$\overline{\boldsymbol{\alpha}}_x(\theta) = \boldsymbol{\alpha}_x \cdot f_x(\theta), \quad \overline{\boldsymbol{\alpha}}_y(\theta) = \boldsymbol{\alpha}_y \cdot f_y(\theta),$$
$$\overline{\boldsymbol{\alpha}}_z(\theta) = \boldsymbol{\alpha}_z \cdot f_z(\theta) \tag{16}$$

To designate the mode in question when referring to a
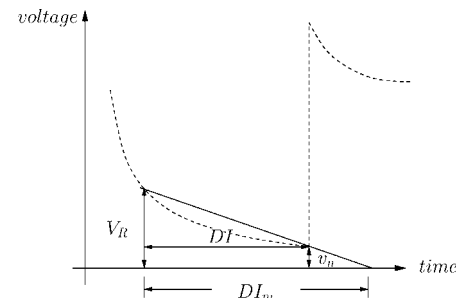
Fig. 8 *DI linearisation*

Table 1: Function definitions for CLHA $\mathcal{A}_2$

	HH	LRd	NNR
$V_T(\theta)$	26	44.5	$39 + 9.7742\theta$
$V_O(\theta)$	106.5	$131.1 - 80.1\sqrt{\theta}$	$106.4 - 133.57\theta^2$
$V_R(\theta)$	30	30	$22 + 10.1091\theta$
$f_x^0(\theta)$	1	1	$1 + \theta$
$f_y^0(\theta)$	1	1	$1 + \theta$
$f_z^0(\theta)$	1	1	$1 + \theta$
$f_x^3(\theta)$	1	1	1
$f_y^3(\theta)$	1	$0.29e^{62.89\theta} + 0.70e^{-10.99\theta}$	$1 + 0.5798\theta$
$f_z^3(\theta)$	1	1	1

specific α or f, we shall henceforth denote them with superscript i, $0 \le i \le 3$, corresponding to modes FR, ST, UP and EP, respectively. The use of this convention can be seen, for example, in Table 1, where the definitions of functions f_x, f_y and f_z for modes FR ($i = 0$) and $EP(i = 3)$ and different cell types (HH, LRd, NNR) are given.

Note how θ influences the shape of the AP within these two modes. The larger the value of θ, the steeper and therefore the shorter the AP. Moreover, although θ is a linear approximation of the DI, the APD depends on θ (and therefore the DI) in a nonlinear way, as θ appears as an exponent in one of the terms of the analytic solution.

To model the dependency of the threshold voltage V_T and overshoot voltage V_O on the DI, we replace constants V_T and V_O with cycle-constant functions $V_T(\theta)$ and $V_O(\theta)$. Their definitions are also given in Table 1. Putting it all together, we obtain the CLHA $\mathcal{A}_2$ shown in Fig. 9.

6.2 Formal definition of the CLHA model

Given an HA $\mathcal{A} = (X, G, \text{init}, \text{inv}, \text{flow}, \text{jump}, \text{event})$, we say that $\mathcal{A}$ is cycle-linear if the following conditions hold.

- The set of variables X is partitioned into a vector $\vec{x}$ of continuous variables and a vector $\boldsymbol{\theta}$ of discrete variables.
- There exists a simple cycle within the control-flow graph $G = (V, E)$ that includes all the vertices in V.
- $\boldsymbol{\theta}$ is updated by all jumps to the initial mode.
- For a fixed θ and for each mode $v \in V$, flow(v) is an LTI system of the form $x = \boldsymbol{\alpha}(\theta)x + \boldsymbol{\beta}(\theta)u$, where u is the input.
- For each mode $v \in V$, inv(v) is a (linear) predicate of the form $x\#\gamma(\theta)$, where $\#$ is one of $\{\le, \ge, <, >\}$ and $\vec{\gamma}(\theta)$ is a constant vector.
- For each switch $e \in E$, jump(e).guard is a predicate having the same form as that of an invariant.
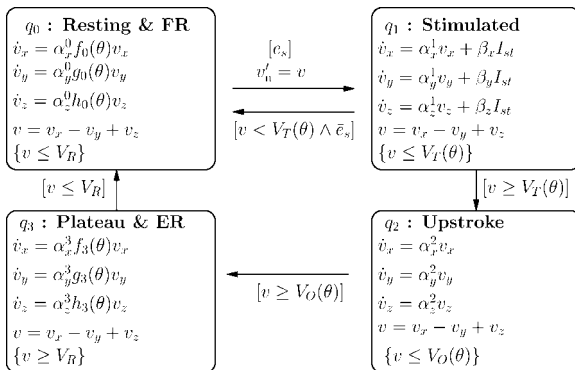
Fig. 9 *CLHA model of excitable cells*

7 Fitting the CLHA model to excitable-cell models

In this section, we demonstrate the versatility of the CLHA model by fitting its parameters to successfully capture the AP morphology and restitution of three popular mathematical models of excitable cells: HH [13], dynamic Rd [14] and NNR.

Fitting the flow parameters of the CLHA excitable-cell model to a specific mathematical model involves the following two-step procedure: (1) Using a single representative AP, with θ set to 0, fit parameters α_w^i, β_w^i, $0 \le i \le 3$, $w \in \{x, y, z\}$. (2) Apply the well-known S1S2 protocol under varying frequencies to obtain a sequence of (DI, APD) pairs, which is then used to fit cycle-constant functions $f(\theta)_w^i$, $0 \le i \le 3$, $w \in \{x, y, z\}$, $V_O(\theta)$ and $V_T(\theta)$. Prior to executing step (2), we 'guess' the form of these θ-related functions; the guiding principle here is to use elementary functions that take into account any extreme values these cycle-constant function may assume.

For example, consider $V_O(\theta)$ in the LRd model. In this case, V_O, the overshoot voltage, varies significantly from AP to AP, attaining a maximum value of 131.1 when $\theta = 0$ and a minimum value of 50.1 when $\theta = 1$. Choosing $V_O(\theta)$ to be the function $131.1 - 80.1\sqrt{(\theta)}$ ensures that V_O attains its proper maximum and minimum values over the range of APs used during the fitting process.

Curve fitting was performed using the unconstrained nonlinear optimisation routines included in the MATLAB Optimisation Toolbox [34]. At each time step, target voltages derived via numerical integration of the HH, LRd and NNR models are compared with the output from the CLHA model, also obtained via numerical integration. A time step of 0.005 ms was chosen to ensure convergence of the implementation of the Euler method underlying the numerical-integration method. The goal of the optimisation routines is to minimise the overall error, which is computed as the sum of the squares of the difference between the outputs of the CLHA model and the target voltages.

Although the optimisation routines we used for curve fitting are completely automatic, the results they produce depend on the initial values supplied to them. In our case, we used a trial-and-error procedure to determine the initial values that resulted in a satisfactory fit. The initial values we ultimately used are available upon request.

The functions and parameters we obtained using our fitting procedure are summarised in Tables 1 and 2.

For a single AP, a comparison of our CLHA model with HH, LRd and NNR is shown in Fig. 10. In the figure, solid lines represent the values obtained via numerical integration of the original nonlinear systems, whereas the dashed lines represent the values obtained via numerical integration of

Table 2: Parameter values for CLHA $\mathcal{A}_2$

	HH	LRd	NNR		HH	LRd	NNR
α_x^0	-0.1770	-0.0087	-0.0647	α_x^2	2.4323	-0.0069	0.3518
α_y^0	-10.7737	-0.1909	-0.0610	α_y^2	3.4556	0.0759	0.0395
α_z^0	-2.7502	-0.1904	-0.0118	α_z^2	2.8111	6.8265	0.0395
α_x^1	0.3399	-0.0236	-0.0473	α_x^3	-1.4569	-0.0332	-0.0087
α_y^1	4.5373	-0.0455	-0.0216	α_y^3	0.0339	0.0280	0.0236
α_z^1	0.0732	-0.0129	-0.0254	α_z^3	-0.9904	0.0020	0.0087
β_x	-3.6051	0.7772	0.7404	β_z	4.9217	0.2766	0.0592
β_y	0.0284	0.0589	0.0869				
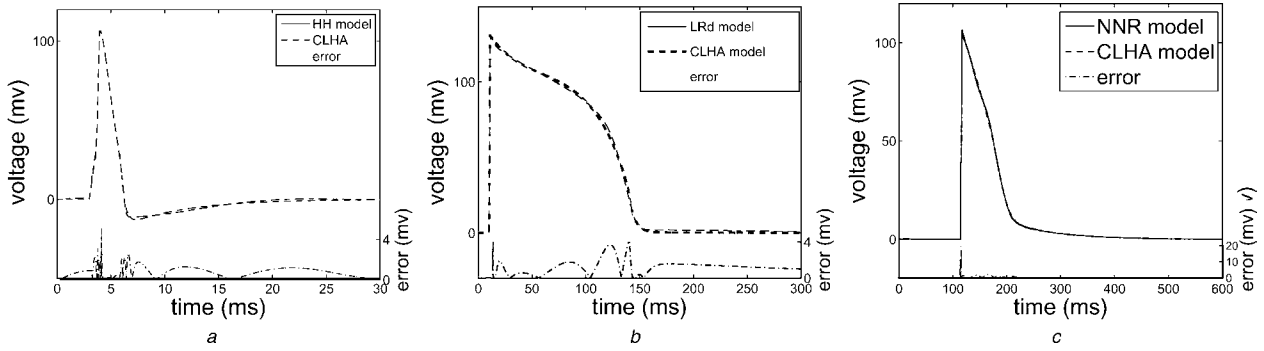
Fig. 10 *AP comparison of CLHA*
a With HH
b With LRd
c With NNR
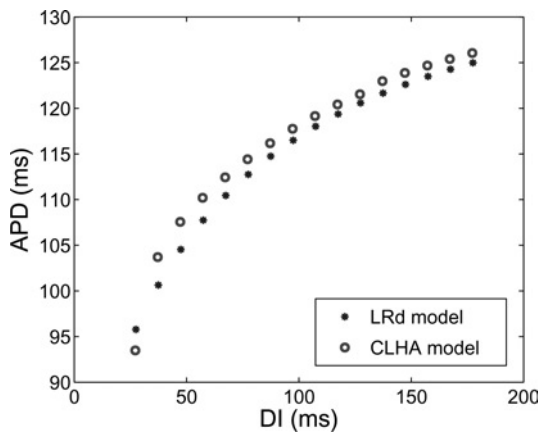
Fig. 11 *Restitution comparison with LRd*

the corresponding CLHA automaton. Fig. 11 compares the restitution functions of the CLHA and LRd models, when pacing the cell with different frequencies. It can be seen that we obtain a nonlinear dependence consistent with that observed for the nonlinear models and also with that observed in live cells.

8 Conclusions

We proposed the use of HA, in general, and CLHAs, in particular, as a general framework for contemporary models of excitable cells. Representing the complex response of these cells with piecewise-linear HA permits fully analytical solutions in the different phases of the excitation cycle, thus providing a framework for analytical analysis regardless of system complexity. Additionally, the piecewise linearisation of the system and the simplified description increase computational efficiency without abstracting away essential system features. Moreover, a cycle-linear model of a dynamical system enjoys both the computational efficiency of a linear model and the descriptive power of a nonlinear one, making it more amenable to formal analysis (e.g. stability analysis) than its nonlinear counterpart.

We illustrated the cycle-linear approach by modelling the behaviour of excitable cells. In doing so, we succeed in capturing the AP morphology and its adaptation to pacing frequency. The method is, however, generally applicable to systems where some level of periodicity plus adaptation is observed. Furthermore, we have shown how to recast two popular approximation models as HA. The resulting graphical representations are easier to understand while still remaining a fully formal model.

Ongoing and future work includes exploring the possibility of associating physiological meaning to the internal state variables v_x, v_y and v_z of our CLHA model. Another direction is to apply formal analysis to our CLHA models of excitable cells in order to study their fundamental properties, including stability, observability and safety (prevention of arrhythmia). We also plan to improve model's computational efficiency using analytical solutions for the linear differential equations within a CLHA mode, thereby eliminating slow iterative integration.

9 Acknowledgment

IET Syst. Biol., Vol. 2, No. 1, January 2008

31

10 References

1 Henzinger, T.A.: 'The theory of hybrid automata'. Proc. 11th IEEE Symp. Logic in Computer Science, 1996, pp. 278–293

2 Varaiya, P.: 'Smart cars on smart roads: problems of control', *IEEE Trans. Autom. Control*, 1993, **38**, (2), pp. 195–270

3 Deshpande, A., Godbole, D., Göllü, A., and Varaiya, P.: 'Design and evaluation of tools for automated highway systems', Hybrid systems III', LNCS 1066, (Springer-Verlag, 1996), pp. 138–148

4 Livadas, C., Lygeros, J., and Lynch, N.A.: 'High-level modelling and analysis of TCAS'. Proc. IEEE Real-Time Systems Symp., 1999, pp. 115–125

5 Lygeros, J., Pappas, G.J., and Sastry, S.: 'An approach to the verification of the center-tracon automation system'. HSCC'98 Proc. First Int. Workshop on Hybrid Systems, London, UK, 1998, (Springer-Verlag), pp. 289–304

6 Balluchi, A., Benvenuti, L., Benedetto, M.D.D., Pinello, C., and Sangiovanni-Vincentelli, A.L.: 'Automotive engine control and hybrid systems: challenges and opportunities', *Proc. IEEE*, 2000, **88**, (7), pp. 888–912

7 Alur, R., Grosu, R., Hur, Y., Kumar, V., and Lee, I.: 'Modular specifications of hybrid systems in charon'. Hybrid Systems: Computation and Control, Third Int. Workshop, 2000, vol. LNCS 1790, pp. 6–19

8 Maler, O., and Yovine, S.: 'Hardware timing verification using KRONOS'. 7th IEEE Israeli Conf. on Computer Systems and Software Engineering, IEEE Computer Society Press, 12–13 June 1996, pp. 23–29

9 Ghosh, R., and Tomlin, C.J.: 'Lateral inhibition through delta-notch signaling: a piecewise affine hybrid model'. Hybrid Systems: Computation and Control: 4th Int. Workshop, Lecture Notes in Computer Science, vol. 2034, Springer-Verlag, Rome, Italy, 2001

10 Milner, R.: 'Communication and concurrency, international series in computer science' (Prentice-Hall, 1989)

11 Biktashev, V.N.: 'A simplified model of propagation and dissipation of excitation fronts', *Int. J. Bifurcation Chaos*, 2003, **13**, pp. 3605–3619

12 Fenton, F., and Karma, A.: 'Vortex dynamics in 3d continous myocardium with fiber rotation: filament instability and fibrillation', *CHAOS*, 1998, **8**, pp. 20–47

13 Hodgkin, A.L., and Huxley, A.F.: 'A quantitative description of membrane currents and its application to conduction and excitation in nerve', *J. Physiol*, 1952, **117**, pp. 500–544

14 Luo, C.H., and Rudy, Y.: 'A dynamic model of the cardiac ventricular action potential: I. simulations of ionic currents and concentration changes', *Circuits. Res.*, 1994, **74**, pp. 1071–1096

15 Ye, P., Entcheva, E., Grosu, R., and Smolka, S.A.: 'Efficient modeling of excitable cells using hybrid automata'. Proc. 3rd International workshop on computational Methods in Systems Biology, Edinburgh, UK, 2005, pp. 216–227

16 Ye, P., Entcheva, E., Smolka, S.A., True, M., and Grosu, R.: 'Hybrid automata as a unifying framework for modeling cardiac cells'. Proc. EMBC, 2006

17 Ye, P., Entcheva, E., Smolka, S.A., True, M., and Grosu, R.: 'A cycle-linear approach to modeling action potentials'. Proc. EMBC, 2006

18 Antoniotti, M., Piazza, C., Policriti, A., Simeoni, M., and Mishra, B.: 'Taming the complexity of biochemical models through bisimulation and collapsing: theory and practice', *Theory. Comput. Sci.*, 2004, **325**, (1), pp. 45–67

19 Alur, R., Dang, T., and Ivancic, F.: 'Reachability analysis of hybrid systems via predicate abstraction'. HSCC, 2002, pp. 35–48

20 Ghosh, R., and Tomlin, C.J.: 'Symbolic reachable set computation of piecewise affine hybrid automata and its application to biological modeling: Delta-notch protein signaling', *IEE Trans. Syst. Biol.*, 2004, **1**, (1), pp. 170–183

21 Dumas, J.G., and Rondepierre, A.: 'Modeling the electrical activity of a neuron by a continuous and piecewise affine hybrid system'. Hybrid Systems: Computation and Control, 2003, pp. 156–171

22 Belta, C., Schug, J., and Dang, T.: 'Stability and reachability analysis of a hybrid model of luminescence in the marine bacterium vibrio fischeri'. 40th IEEE Conf. Decision and Control, 2001, vol. 1, pp. 869–874

23 FitzHugh, R.: 'Impulses and physiological states in theoretical models of nerve membrane', *Biophys. J.*, 1961, **1**, pp. 445–467

24 Nagumo, J., Arimoto, S., and Yoshizawa, S.: 'An active pulse transmission line simulating nerve axon', *Proc of the IRE*, 1962, **50**, (10), 2061–2070

25 Mckean, H.P.: 'Nagumo's equation', *Adv. Math.*, 1970, **4**, pp. 209–223

26 Tikhonov, A.N.: 'Systems of differential equations, containing small parameters at the derivatives', *Mat. Sbornik*, 1952, **31**, (3), pp. 575–586

27 Pontryagin, L.S.: 'The asymptotic behaviour of systems of differential equations with a small parameter multiplying the highest derivatives', *Izv. Akad. Nauk SSSR, Ser. Mat.*, 1957, **21**, (5), pp. 107–155

28 Suckley, R., and Biktashev, V.N.: 'Comparison of asymptotics of heart and nerve excitability', *Phys. Rev. E*, 2003, **68**, 011902, 1–15

29 Biktasheva, I., Simitev, R., Suckley, R., and Biktashev, V.N.: 'Asymptotic properties of mathematical models of excitability', *Phil. Trans. Roy. Soc. A: Math. Phys. Eng. Sci.*, 2006, **364**, pp. 1283–1298

30 Courtemanche, M., Ramirez, R.J., and Nattel, S.: 'Ionic mechanisms underlying human atrial action potential properties: insights from a mathematical model', *Am. J. Physiol.*, 1998, **275**, pp. 301–321

31 Simitev, R.D., and Biktashev, V.N.: 'Conditions for propagation and block of excitation in an asymptotic model of atrial tissue', *Biophys. J.*, 2006, **90**, pp. 2258–2269

32 True, M., Entcheva, E., Smolka, S.A., Ye, P., and Grosu, R.: 'Efficient event-driven simulation of excitable hybrid automata'. Proc. EMBC, 2006

33 Grosu, R., Mitra, S., Ye, P., Entcheva, E., Ramakrishnan, I., and Smolka, S.A.: 'Learning cycle-linear hybrid automata for excitable cells'. Hybrid Systems: Computation and Control, LNCS, vol. 4416 (Springer, Pisa, Italy, 2007), pp. 245–258

34 'MATLAB Online Reference Documentation', http://www.mathworks.com/access/helpdesk/help/toolbox/optim/, 2007

32

IET Syst. Biol., Vol. 2, No. 1, January 2008